This is the accepted manuscript made available via CHORUS. The article has been published as:

Self-Consistent Tilted-Axis-Cranking Study of Triaxial Strongly Deformed Bands in ^{158}Er at Ultrahigh Spin

Yue Shi, J. Dobaczewski, S. Frauendorf, W. Nazarewicz, J. C. Pei, F. R. Xu, and N. Nikolov

Phys. Rev. Lett. **108**, 092501 — Published 28 February 2012

DOI: 10.1103/PhysRevLett.108.092501

Self-consistent tilted-axis-cranking study of triaxial strongly deformed bands in ^{158}Er at ultrahigh spin

Yue Shi,[1,2,3,4] J. Dobaczewski,[5,4] S. Frauendorf,[6] W. Nazarewicz,[2,3,5] J.C. Pei,[7,2,3] F.R. Xu,[1] and N. Nikolov[2]

[1] *State Key Laboratory of Nuclear Physics and Technology, School of Physics, Peking University, Beijing 100871, China*
[2] *Department of Physics and Astronomy, University of Tennessee, Knoxville, Tennessee 37996, USA*
[3] *Physics Division, Oak Ridge National Laboratory, Post Office Box 2008, Oak Ridge, Tennessee 37831, USA*
[4] *Department of Physics, PO Box 35 (YFL), FI-40014 University of Jyväskylä, Finland*
[5] *Institute of Theoretical Physics, Faculty of Physics, University of Warsaw, ul. Hoża 69, PL-00681 Warsaw, Poland*
[6] *Department of Physics, University of Notre Dame, Notre Dame, Indiana 46556, USA*
[7] *Joint Institute for Heavy-Ion Research, Oak Ridge, Tennessee 37831, USA*

Stimulated by recent experimental discoveries, triaxial strongly deformed (TSD) states in ^{158}Er at ultrahigh spins have been studied by means of the Skyrme-Hartree-Fock model and the tilted-axis-cranking method. Restricting the rotational axis to one of the principal axes – as done in previous cranking calculations – two well-defined TSD minima in the total Routhian surface are found for a given configuration: one with positive and another with negative triaxial deformation γ. By allowing the rotational axis to change direction, the higher-energy minimum is shown to be a saddle point. This resolves the long-standing question of the physical interpretation of the two triaxial minima at a very similar quadrupole shape obtained in the principal-axis-cranking approach. Several TSD configurations have been predicted, including a highly deformed band expected to cross lesser elongated TSD bands at the highest spins. Its transitional quadrupole moment $Q_t \approx 10.5\,$eb is close to the measured value of $\sim$11 eb; hence, it is a candidate for the structure observed in experiment.

PACS numbers: 21.60.Jz, 21.10.Re, 21.10.Ky, 27.70.+q

While the majority of nuclei have axially symmetric shapes, evidence for triaxial nuclear deformations has been elusive. The clearest signatures come from the gamma-ray spectroscopy of rotating nuclei. The deformation of a quantum object, such as molecule or atomic nucleus, enables the system to specify an orientation. The quantized motion of this degree of freedom generates the sequences of rotational levels - the rotational bands [1, 2]. If the system is triaxial, the associated rotational bands show specific features that allow for distinguishing it from an axial one. In the case of nuclei, the appearance of the wobbling [1, 3, 4] and spin-chirality [2, 5] rotational modes are experimental signatures of triaxiality.

Triaxial shapes are expected to appear more frequently at high spin because of the tendency of aligned high-j quasiparticles to drive rotating nuclei towards triaxiality due to their spatial density distributions [6, 7]. In addition, pairing correlations – which generally favor more symmetric shapes – are quenched at high spins and enhance the high-j alignment effect [8]. Consequently, with increasing spin, nuclei are predicted to go through non-axial shapes before they eventually fission (see, e.g., [9]).

Recent experiments [10–16] have reached ultrahigh spins of about $65\hbar$ in nuclei around ^{158}Er. It has been observed that with increasing angular momentum, the rotational bands terminate and nuclei assume weakly deformed oblate shapes, as evidenced by the irregular level spacings. At ultrahigh spins they return to collective rotation characterized by regular rotational bands, consistent with the early prediction [17]. Cranked Nilsson-Strutinsky calculations suggest that the observed bands in ^{158}Er are based on one of the three triaxial strongly deformed (TSD) minima in the potential-energy surface (see Ref. [16] and references cited therein). For the lowest minimum TSD1, with positive γ, the calculated value of the transitional quadrupole moment $Q_t \approx 7.5\,$eb considerably underestimates the observed value of $\sim 11\,$eb [16]. This has led to the suggestion that the observed band in ^{158}Er may be associated with either the minimum TSD2, which has a similar quadrupole deformation parameter ε_2 as TSD1 but negative γ, or with the band TSD3, which has a larger triaxial deformation [16].

Most of the existing high-spin calculations in the mass-160 region assume that the axis of rotation coincides with one of the principal axes of the triaxial potential, which is commonly referred to as principal-axis cranking. The cranked Nilsson-Strutinsky calculations use the microscopic-macroscopic method, which combines a shell correction derived from a phenomenological potential with the deformation energy of a rotating liquid drop [17–19]. It is common to choose the x-axis as the rotational axis and let the triaxiality parameter cover the range $-120^\circ \leq \gamma \leq 60^\circ$. In the Lund convention, which we adopt in this Letter, the three sectors $[-120^\circ, -60^\circ]$, $[-60^\circ, 0^\circ]$, and $[0^\circ, 60^\circ]$ represent the same triaxial shapes but represent rotation about the long, medium and short axis, respectively. The TSD1

and TSD2 minima in the cranked Nilsson-Strutinsky calculations [16] correspond to similar values of ε_2 and $|\gamma|$ which means that their shapes are nearly the same. The opposite sign of γ means that TSD1 rotates about the short axis and TSD2 about the medium axis. This raises the question of their physical interpretation, e.g., whether the higher of the two minima obtained in the principal-axis-cranking approach is stable with respect to a reorientation of the rotational axis.

In this Letter we address this question by means of the tilted-axis-cranking method [20, 21], which considers the general orientation of the axis of rotation with respect to the principal axes of the nuclear quadrupole moment. We investigate the structure of ultrahigh-spin TSD minima in ^{158}Er by using two approaches: the shell-correction tilted-axis-cranking method (SCTAC) [20], which is based on the phenomenological Nilsson potential, and, for the first time, the three-dimensional self-consistent Skyrme-Hartree-Fock (SHF) version of tilted-axis cranking (SHFTAC) developed in Ref. [22]. Employing a fully self-consistent rotating mean field – including the full rotational response due to cranking – is expected to improve the reliability of calculations in the realm of ultrahigh-spin states.

SHFTAC is based on the symmetry-unrestricted solver HFODD (v2.49s) [23], which has been successfully applied to the description of chiral bands in ^{132}La [22]. In the particle-hole channel, we use the Skyrme energy density functionals SkM* [24] and SLy4 [25], the latter of which has been supplemented with Landau parameters (SLy4$_{\rm L}$) [26, 27]. The total energy of the system $\mathcal{E}$ is obtained by integrating the total energy density over spatial coordinates. We have used 1,000 deformed harmonic oscillator basis states with $\hbar\omega_\perp = 10.080$ MeV and $\hbar\omega_\parallel = 7.418$ MeV. At ultrahigh spins, pairing is negligible; hence, it has been ignored in SCTAC and SHFTAC. As discussed in earlier SHF principal-axis-cranking calculations [7], quadrupole polarization at high spin – both axial and triaxial – is very well described by unpaired theory. The SCTAC calculations give a strong increase

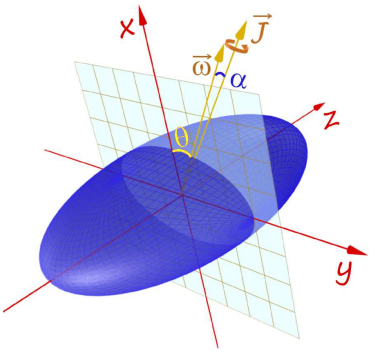

FIG. 1: (Color online) Schematic picture of a TSD shape. The angles θ (between the x-axis and the rotational axis) and α (between $\boldsymbol{\omega}$ and $\boldsymbol{J}$) are defined in the $x-y$ plane. The short, medium, and long axes are denoted by x, y, and z, respectively; that is, the plotted shape corresponds to $\gamma > 0$.

of the Routhian $\mathcal{E}^\omega \equiv \mathcal{E} - \boldsymbol{\omega}\cdot\boldsymbol{J}$ when the rotational axis is tilted toward the z-axis. For this reason we restrict the numerically extensive SHFTAC calculation to the $x-y$ plane spanned by the short and medium axes. The tilt angle θ of the rotational axis is measured with respect to the short axis, as illustrated in Fig. 1.

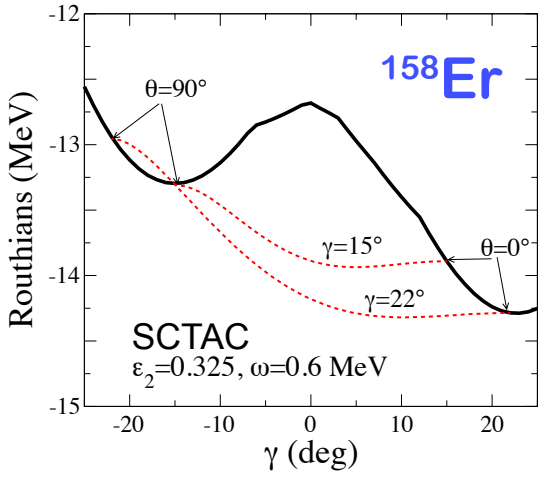

FIG. 2: (Color online) Lowest Routhians in ^{158}Er calculated by means of SCTAC (Nilsson potential) at fixed ε_2 and ω as a function of γ for rotation about the x-axis (solid line) compared to those calculated at $\gamma = 15^\circ$ and 22° as functions of θ (dashed lines). In the latter case, the Routhians are drawn by uniformly scaling the range of $0^\circ \le \theta \le 90^\circ$ into the corresponding ranges of γ.

Figure 2 shows the results of the SCTAC calculations. If the axis of rotation agrees with one of the principal axes, SCTAC coincides essentially with the cranked Nilsson-Strutinsky results of Ref. [18]. (In SCTAC the Strutinsky renormalization is only carried out for the non-rotational part of the Routhian, whereas in the cranked Nilsson-Strutinsky method the rotational energy is also renormalized.) The equilibrium deformation parameters in SCTAC for rotation about the short axis are $\varepsilon_2 = 0.325$, $\gamma = 22^\circ$ (lower minimum), and for rotation about the medium axis $\varepsilon_2 = 0.31$, $\gamma = -15^\circ$ (higher minimum), which are close to the TSD1 and TSD2 minima of Ref. [16], respectively.

It is clearly seen in Fig. 2 that the principal-axis-cranking minimum at $\gamma = -15^\circ$ becomes a saddle if the rotational axis is allowed to tilt. The dashed lines show how the energies change in a smooth way when tilting the rotational axis from short ($\theta = 0^\circ$) to medium ($\theta = 90^\circ$) while keeping ε_2 and γ constant. *Thus one cannot associate TSD2 with the band observed in ^{158}Er.* In addition, the transition quadrupole moment for the stable minimum TSD1 is ∼8 eb, which is too small as compared with the experimental value of ∼11 eb (see also the discussion in [16]).

In the case of SCTAC, the tilt angle of the rotational axis is defined relative to one of the principal axes of the deformed potential in a straightforward way. In SHF-

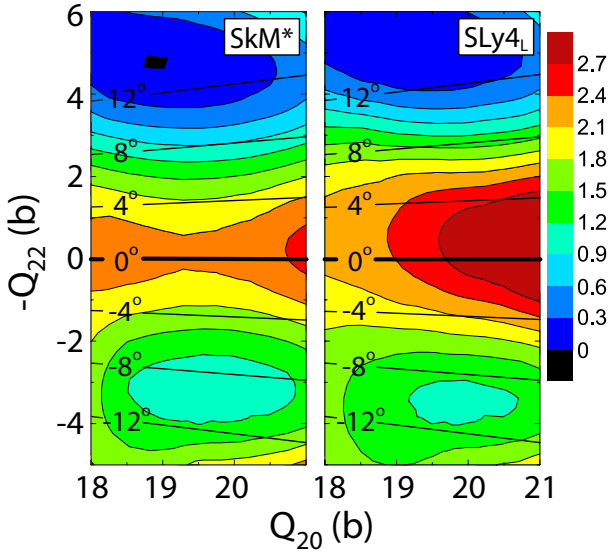

FIG. 3: (Color online) Total Routhian surfaces in the (Q_{20}, Q_{22}) plane for the A-configuration of Table I at $\omega = 0.7$ MeV and $\theta = 0$ (principal-axis cranking) obtained with SkM* (left) and SLy4$_{\rm L}$ (right) functionals. The corresponding values of γ are marked.

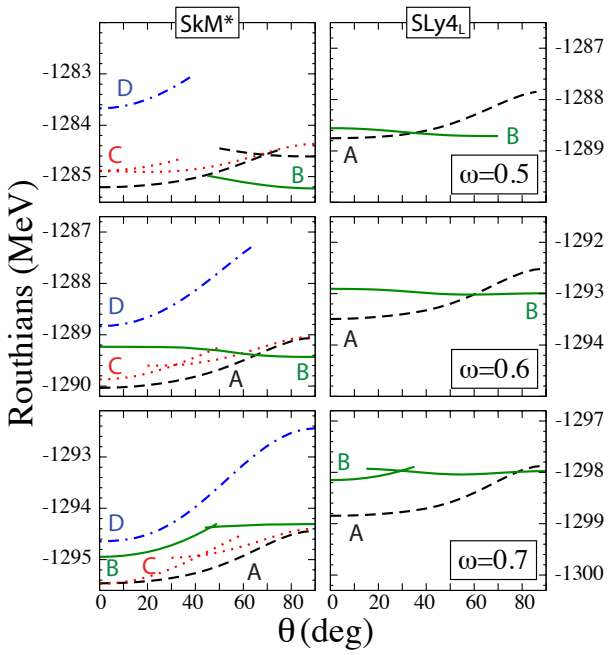

FIG. 4: (Color online) Total Routhians of ^{158}Er as a function of θ at ω=0.5, 0.6, and 0.7 MeV for SkM* (left) and SLy4$_L$ (right) functionals. Dashed, solid, dotted, and dot-dashed lines represent TSD configurations A, B, C, and D, respectively (see Table I). Note that the labeling of the configurations is only valid when $\theta = 0°$ or 90°. Otherwise, the signature is no longer a good quantum number. For the SLy4$_L$ functional, converged solutions for configurations C and D could not be obtained.

TAC calculations, it must be introduced by means of a constraint on the orientation of $\boldsymbol{J}$ along with the constraints $\mathrm{Im}(Q_{22}) = Q_{2\pm1} = 0$ on the orientation of the principal axis of the nucleus defined in terms of the total (mass) quadrupole moment $Q_{2\mu}$. The conditions on the corresponding Lagrange multipliers have been derived by Kerman and Onishi [21]. We use the 2D counterpart of relation (3.6) of Ref. [21], which states that $\boldsymbol{\omega}$ and $\boldsymbol{J}$ are not parallel ($\alpha \neq 0°$) if the Routhian is not at a stationary point. By using the Augmented Lagrangian Method of the HFODD code [23], we have checked that the Kerman-Onishi conditions are obeyed to a high precision for all angles θ. The resulting angles α do not exceed 0.1–0.2°, depending on configuration.

TABLE I: The SHF configurations in ^{158}Er studied in this Letter. Each configuration is described by the number of states occupied in the four parity-signature (π, r) blocks, in the convention defined in Ref. [28], and also by the transition quadrupole moment Q_t. The Q_t values are from the SHF-SkM* calculations at $\omega = 0.6$ MeV and $\theta = 0°$. Q_t is calculated from charge quadrupole moments through the relation $Q_t = Q_{20}^{\rm ch} + \sqrt{\frac{1}{3}} Q_{22}^{\rm ch}$ [7].

	configuration	π	r	Q_t (eb)
A:	$\nu[23,23,22,22] \otimes \pi[17,18,16,17]$	$-$	-1	7.6
B:	$\nu[23,23,22,22] \otimes \pi[17,17,17,17]$	$+$	$+1$	7.7
C:	$\nu[23,24,21,22] \otimes \pi[17,18,16,17]$	$+$	$+1$	7.4
D:	$\nu[23,23,22,22] \otimes \pi[17,17,17,17]$	$+$	$+1$	10.7

In this Letter, we studied four different SHF configurations listed in Table I. They all are expected to appear near yrast around Q_{20}=19 eb. First, in Fig. 3 we show the Routhian surfaces for the A-configuration obtained in the principal-axis-cranking SHF approach at $\omega = 0.7$ MeV and $\theta = 0°$. The Routhians calculated for the two functionals, SkM* and SLy4$_L$, are rather similar. (They are also similar to those of the SCTAC and those of Ref. [16], which have a somewhat smaller barrier of ∼0.7 MeV.) Clearly visible two minima at $\gamma = -\arctan Q_{22}/Q_{20} \approx 14°$ and $-10°$ are well separated by a potential barrier of ∼ 1 MeV at $\gamma \approx 0°$.

In Fig. 4 we allow the rotational axis to tilt ($\theta \neq 0$) by starting from SHF principal-axis-cranking solutions with $Q_{22} \approx -4$ b. [A rotation of this shape around the y-axis ($\theta = 90°$) is equivalent to that of $Q_{22} \approx 4$ b around the x-axis ($\theta = 0°$).] It can be seen that for the configuration A, the minimum that appears in Fig. 3 at $Q_{22} \approx 4$ b ($\gamma \approx -10°$) is unstable with respect to a reorientation of the rotational axis, that is, it represents the saddle-point. On the other hand, the lower minimum, at $\gamma \approx 14°$, remains stable. This is consistent with SCTAC calculations of Fig. 2. A similar situation is predicted for configurations C and D. At ω=0.5 MeV, the configuration B has a minimum at $\theta = 90°$ ($\gamma < 0$), but it becomes θ-unstable at higher rotational frequencies and a minimum at $\theta = 0°$ develops at ω=0.7 MeV. This interesting

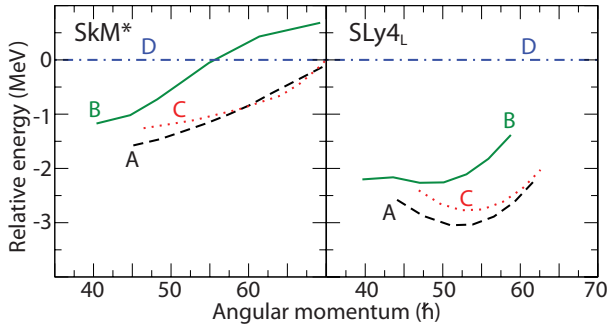

FIG. 5: (Color online) Relative energies of configurations A (dashed), B (solid), and C (dotted) with respect to D (dash-dotted line at 0 MeV).

behavior, together with a discussion of wobbling modes in bands A-D will be discussed in detail in a forthcoming paper.

As seen in Table I, while bands B and D have the same parity-signature occupations, configuration D has much larger deformation: $Q_{20} \approx 29\,\mathrm{b}$, $Q_{22} \approx -6\,\mathrm{b}$ ($\gamma = 12°$). Figure 5 compares the energies of configurations A, B, and C with that of D. For the SkM* functional (left), which has been partly optimized at large deformations, it can be seen that at low spins band D lies about 1 MeV above band B and 1.5-1.8 MeV above bands A and C. Due to its large moment of inertia, band D crosses band B at about $J \approx 55\hbar$ and bands A and C at $J \approx 70\hbar$. As illustrated in Fig. 4, D-configuration is stable against the rotational axis tilting. Table II compares the quadrupole moments of the lowest TSD1 configuration A with those of band D at several values of ω.

Band D is our best candidate for the structure observed in experiment: the calculated $Q_t \approx 10.5\,\mathrm{eb}$ of this configuration well reproduces the experimental value of $\sim$11 eb [16]. (We note that band D has a larger quadrupole moment and smaller γ than band TSD3 of Ref. [16].) While the energy-spin relations of Fig. 5 are not inconsistent with the spin estimates of Ref. [10], the fact that the TSD1 bands A and C do not seem to be seen experimentally, and that the experimental intensity pattern shows an increase in side feeding all the way to the point of decay-out, both suggest that band D should be more favored energetically than predicted. Indeed, we do not expect the relative energies calculated in SHF using current functionals to be precise, as evidenced by appreciable differences between SkM* and SLy4$_\mathrm{L}$ predictions in Fig. 5.

In summary, we have performed, for the first time, tilted-axis-cranking calculations within the self-consistent Skyrme-Hartree-Fock model in which the Kerman-Onishi conditions for triaxial rotation are strictly obeyed. To address the recent puzzling experimental data, we studied the nucleus ^{158}Er at ultrahigh spins. Restricting the direction of the rotational axis to one of the principal axes of the density distribution yields two TSD minima with similar ϵ_2 values but with positive and negative γ deformations, similar to our SCTAC predictions and the results of Ref. [16]. Allowing the rotational axis to tilt away from the principal axes shows, however, that the higher-energy minimum is actually a saddle point; hence, it cannot be associated with a physical state. It is the lower-energy minimum that represents a TSD band. We have thus clarified a long-standing question pertaining to the nature of positive- and negative-γ bands associated with the same intrinsic shape in the principal-axis-cranking approach: the rotation of a well-deformed, slightly triaxial configuration can be either about a short or medium axis, but not about both.

TABLE II: Charge quadrupole moments, transition (charge) quadrupole moments, and angular momenta for bands A and D calculated with SkM*.

Band	ω (MeV)	Q_{20}^{ch} (eb)	$-Q_{22}^{\mathrm{ch}}$ (eb)	Q_t (eb)	J ($\hbar$)
A	0.50	9.0	1.9	7.9	45.1
	0.60	8.7	2.0	7.6	51.6
	0.70	8.4	2.0	7.2	57.3
	0.80	8.1	2.1	6.9	62.8
D	0.40	11.8	2.3	10.5	31.5
	0.50	12.2	2.4	10.8	48.4
	0.60	12.1	2.5	10.7	54.8
	0.70	12.1	2.5	10.6	61.8
	0.80	12.0	2.5	10.5	71.9

Several TSD configurations differing by proton and neutron occupations and quadrupole moments have been investigated. In the angular momentum range of 50–70 $\hbar$, they are predicted to have transition quadrupole moments of 7–8 eb, which are below the measured values of $Q_t \approx 11\,\mathrm{eb}$ [16]. We have identified an excited TSD configuration, band D, with a stable positive-γ minimum, which has a large transition quadrupole moment of $Q_t \approx 10.5\,\mathrm{eb}$ that agrees well with the experimental value. At spins higher than $\sim 55\hbar$, this band – different from structures TSD3 and SD of Ref. [16] – lies close to the less deformed TSD bands, and it is expected to become yrast above $J > 70\hbar$. The experimental intensity pattern suggests that band D should lie lower in energy than predicted by SkM* and SLy4$_\mathrm{L}$ models used in this study; this opens up an interesting direction for future investigations aiming at developing the spectroscopic-quality nuclear energy density functional.

Pertinent and stimulating questions by Mark Riley, and numerous valuable discussions with him, are gratefully acknowledged. This work has been supported by the Natural Science Foundation of China under Grants Nos. 10735010 and 10975006; U.S. Department of Energy under Contract Nos. DE-FG02-96ER40963 (University of Tennessee) and DE-FG02-95ER40934 (University of Notre Dame); Academy of Finland and the University of Jyväskylä within the FIDIPRO programme.

[1] A. Bohr and B.R. Mottelson, *Nuclear Structure* (Benjamin, New York, 1975), Vol. II.
[2] S. Frauendorf, Rev. Mod. Phys. **73**, 463 (2001).
[3] S.W. Ødegård, G.B. Hagemann, D.R. Jensen, M. Bergström, B. Herskind, G. Sletten *et al.*, Phys. Rev. Lett. **86**, 5866 (2001).
[4] D.R. Jensen, G.B. Hagemann, I. Hamamoto, S.W. Ødegård, B. Herskind, G. Sletten *et al.*, Phys. Rev. Lett. **89**, 142503 (2002).
[5] S. Frauendorf and J. Meng, Nucl. Phys. A **617**, 131 (1997).
[6] S. Frauendorf and F.R. May, Phys. Lett. B **125**, 245 (1983).
[7] M. Matev, A.V. Afanasjev, J. Dobaczewski, G.A. Lalazissis, and W. Nazarewicz, Phys. Rev. C **76**, 034304 (2007).
[8] M. Matsuzaki, Y.R. Shimizu, and K. Matsuyanagi, Phys. Rev. C **65**, 041303(R) (2002).
[9] T.R. Werner and J. Dudek, Atom. Tab. Nucl. Dat. Tab. **50**, 179 (1992).
[10] E.S. Paul, P.J. Twin, A.O. Evans, A. Pipidis, M.A. Riley, J. Simpson *et al.*, Phys. Rev. Lett. **98**, 012501 (2007).
[11] N.S. Pattabiraman, Y. Gu, S. Frauendorf, U. Garg, T. Li, B.K. Nayak *et al.*, Phys. Lett. B **647**, 243 (2007).
[12] A. Aguilar, D.B. Campbell, K. Chandler, A. Pipidis, M.A. Riley, C. Teal *et al.*, Phys. Rev. C **77**, 021302(R) (2008).
[13] C. Teal, K. Lagergren, A. Aguilar, D.J. Hartley, M.A. Riley, J. Simpson *et al.*, Phys. Rev. C **78**, 017305 (2008).
[14] J. Ollier, J. Simpson, X. Wang, M.A. Riley, A. Aguilar, C. Teal *et al.*, Phys. Rev. C **80**, 064322 (2009).
[15] J. Ollier, J. Simpson, M.A. Riley, E.S. Paul, X. Wang, A. Aguilar *et al.*, Phys. Rev. C **83**, 044309 (2011).
[16] X. Wang, M.A. Riley, J. Simpson, E.S. Paul, J. Ollier, R.V.F. Janssens *et al.*, Phys. Lett. B **702**, 127 (2011).
[17] J. Dudek and W. Nazarewicz, Phys. Rev. C **31**, 298 (1985).
[18] T. Bengtsson and I. Ragnarsson, Nucl. Phys. A **436**, 14 (1985).
[19] A.V. Afanasjev, D.B. Fossan, G.J. Lane, and I. Ragnarsson, Phys. Rep. **322**, 1 (1999).
[20] S. Frauendorf, Nucl. Phys. A **557**, 250c (1993); Nucl. Phys. A **677**, 115 (2000).
[21] A.K. Kerman and N. Onishi, Nucl. Phys. A **361**, 179 (1981).
[22] P. Olbratowski, J. Dobaczewski, J. Dudek, and W. Płóciennik, Phys. Rev. Lett. **93**, 052501 (2004).
[23] N. Schunck, J. Dobaczewski, J. McDonnell, W. Satuła, J.A. Sheikh, A. Staszczak *et al.*, Comput. Phys. Commun. **183**, 166 (2012).
[24] J. Bartel, P. Quentin, M. Brack, C. Guet, and H.-B. Håkansson, Nucl. Phys. A **386**, 79 (1982).
[25] E. Chabanat, P. Bonche, P. Haensel, J. Meyer, and R. Schaeffer, Nucl. Phys. A **635**, 231 (1998).
[26] M. Bender, J. Dobaczewski, J. Engel, and W. Nazarewicz, Phys. Rev. C **65**, 054322 (2002).
[27] H. Zduńczuk, W. Satuła, and R.A. Wyss, Phys. Rev. C **71**, 024305 (2005).
[28] J. Dobaczewski and J. Dudek, Comput. Phys. Commun. **131**, 164 (2000).